



Application of ultrathin asphalt overlay technology with 4.75-mm nominal maximum aggregate size

Lin Li* and Qiang Li

Central expressway management (Shanxi). Co, Ltd. 030006, Taiyuan, Shanxi, China.

LiLinME@outlook.com

Abstract. Ultra-thin asphalt overlay (UAO), described as an ultrathin overlay, is formulated of hot-mix asphalt placed on a polymer-modified asphalt emulsion tack coat. The total wearing surface thickness of UAO ranges from 5 mm to 15 mm, ensuring thorough waterproofing of the pavement and high skid resistance. This study focused on the constructability and performance of UAO treatments with three aggregate types, including open-graded, half-open-graded, and dense-graded. Special specimens are made for laboratory tests to compare the performance of UAOs, all laboratory results, trial sections survey, and core samples tests are consistent with the previous laboratory tests. UAO treatment with half open-graded aggregate does best on mechanical performance and open-graded aggregate seems to be not suitable for UAO treatment. However, a dense-graded mixture has higher water stability than a half-open-graded mixture, which may be due to both aggregate gradation and asphalt. By comparative analysis of the mixture and trial section performance, asphalt and interlayer oil properties are found to have no significant influence on UAO performance. The gradation is the main factor. The performance of anti-noise, skid resistance, and the ability to restore pavement smoothness also mainly depends on the gradation. Half-open-graded is found to be the most suitable mixture for UAO, but the pull-off test results and UAO conditions in the field after a short period imply that the half-open gradation is sensitive to water. Water stability and durability should be verified during the design of the UAO mixture, especially for rainy areas.

Keywords: preventative maintenance; ultra-thin asphalt overlay; bond property; water stability; rutting test; skid resistance; aggregate gradation

1 Introduction

During the history of thin overlay, there are many names with different thickness ranges and functions, such as very thin overlay (VTO), ultrathin multi-functional overlay (UMO), ultra-thin bituminous overlays (UTBO), ultra-thin bonded wearing course (UTBWC), and porous ultra-thin overlay (PUTO), etc. The original expressions of the thin overlay from citations are used below.

Overlay thickness (50.8 mm to 127 mm) greatly impacts the IRI deterioration rate and there is no significant difference between the deterioration rates of IRI when two

test sections only differ in overlay materials [1]. The surface thickness in an equivalent structure depends on the overlay thickness and the bonding condition between the overlay and existing pavement [2]. There are no significant differences in pavement performance between using gap-graded asphalt rubber concrete and dense-graded asphalt concrete as a thin overlay layer (25mm to 35 mm) [3]. UTBO (9.5 mm to 19 mm) is found to have no consistent improvement in rutting conditions and a sharp drop-off in the effectiveness in mitigating transverse and fatigue cracking [4]. According to the above literature research, the changes in thickness are proved to have an impact on the performance of the overlay, but the characteristics of the mixture show no influence on the performance of the overlay.

Some engineers have developed their overlays and verified the performance: VTO (20 mm) is proposed as an appropriate material for urban pavements as it provides good durability and resistance to the propagation of defects with higher skid resistance, and lower susceptibility to moisture, temperature, and aging by oxidation compared to a traditional 35 mm thick overlay. However, the macrotexture depth of VTO is lower [5]. VTO with a thickness of 19 mm is used to replace micro-surfacing and has been found successful in overlaying pavements with fairly wide cracks or shallow rutting [6]. UMO (12 mm to 15mm) has shown a remarkable capacity to protect the asphalt pavement surface, including sealing cracks, improving scratch resistance, maintaining the stiffness of the materials subjected to thermal stress, and reducing the service temperature of the asphalt [7]. PUTO is designed as an OGFC mixture combining skid resistance and drainage functions, laboratory tests imply gradation plays a major role in its performance and strength [8]. The Georgia Department of Transportation (DOT) has developed and implemented a new pavement preservation method that uses micro-milling in conjunction with a thin overlay for the cost-effective replacement of a deteriorated, thin, open-graded surface layer (19 mm to 32 mm) [9]. The simulation predicts thin-lift overlays (25-mm-thick asphalt) and the traditional 50-mm-thick rehabilitation practice both will perform satisfactorily during their expected design life, but the life cycle cost analysis (LCCA) indicates that the practice of using the thin-layer preservation technique can reduce both the agency's and users' costs compared with the conventional 50-mm-thick rehabilitation practice [10].

The failures of thin overlays have been summarized and experimentally analyzed in some studies. Reflective cracking is found the dominant distress of thin overlay projects [11]. Top-down cracking is significantly delayed by thin overlay, but once the pavement sections are aged and brittle, the treatment would be invalid [12]. Pavement sections with UTBWC (30 mm) are reported to experience a loss of friction resulting in several accidents within the first year of construction, and the reason found is the excess binder in the tack coat [13]. UTBWC (16 mm) is found to be not good at reducing noise [14]. The aggregate skeleton gradation is important in the design of asphalt concrete mixtures used in thin overlays to achieve desirable cracking performance. The mixtures with a reduced NMA and low content of fine aggregates are found to be a further improvement of overlay toughness [15]. 4.75-mm SMA is more efficient and cost-effective than 9.5-mm dense-graded and 12.5-mm SMA with a lower noise level, higher friction, and equivalent ride quality [16]. The nominal maximum aggregate size (NMA) recommended for surface thickness less than 20 mm is 4.75 mm [17].

This paper aims to confirm the feasibility and the essential design indicators of ultrathin asphalt overlay (UAO) (5 mm to 15 mm) as a preventive maintenance treatment to add structural capacity, improve ride, enhance skid resistance, reduce noise, seal cracks, and improve drainage. Specifically, the initial part of this paper describes the properties that should be part of the UAO mix design method to guarantee the adequate performance of the mixture in terms of durability and functionality. Next, laboratory test results and pavement performance of trial sections are discussed to figure out laboratory test indicators. It should be noted that there are other relevant aspects associated with the performance of UAO mixtures (e.g., construction techniques, structural contribution, and environmentally-related degradation processes) that are out of the scope of this paper, the main focus of this paper is aggregate types and key test indicators for UAO treatments.

2 Materials and Method

Three types of UAO treatments with different aggregate gradations were chosen for laboratory and field tests. LFT is one brand of the open-graded mixture (similar to OGFC-4.75), GT is a dense-graded (similar to AC-4.75) mixture and RL is a half open-graded (similar to SMA-4.75) mixture. The properties of materials are tested to figure out the best combination of each mixture group. Property indexes of asphalt include penetration, softening point, ductility, and elastic restitution percent, property indexes of interlayer oil include viscosity, storage stability, and sieve residue. Laboratory tests include Marshall stability and Cantabro stripping with Marshall specimens, diagonal shear test and end tensile test with simulated UAO specimens, end tensile test and cycle rutting test with core specimens to analyze the mechanical performance. Water stability performances of GT and RL are tested by freeze-thaw splitting tests, immersion Marshall tests and immersion Hamburg Wheel Tracking stability tests. Trial sections were constructed and pavement conditions were surveyed after one year, macrotexture depth (MTD), friction coefficient (BPN), permeability coefficient, and maximum clearance were used for anti-noise, skid resistance, waterproofing permeability, and roughness assessment separately. Comparative analysis of different types of UAOs, correlation analysis of material properties, and performance indexes are used to determine the critical factors in the success of UAO design.

2.1 Asphalt, interlayer oil, and aggregate gradations

Tests for asphalt include (1) the penetration test (T0604-2011), (2) the ductility test (T0605-2011), (3) softening point test (ring and ball method) (T0606-2011), and (4) the elastic recovery test (T0662-2011) [18], results are shown in Table 1. Tests for interlayer oils were carried out according to T0651, T0624, T0652, and T0655 for emulsified asphalts [18], and the results are shown in Table 2.

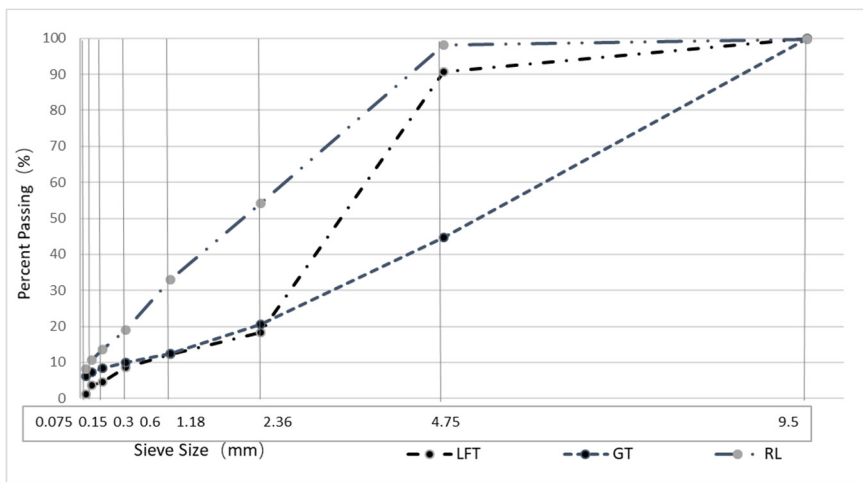
Gradations of the three mixtures are shown in Figure 1, and asphalt aggregate ratios of the three mixtures (LFT, GT, and RL) are 5.9%, 7.5%, and 6.5% respectively.

Table 1. Test results of asphalt

Test items	Sample types		
	LFT	GT	RL
Penetration (0.1 mm)	49	48	69
Ductility (10°C) (cm)	9.6	/	/
Ductility (5°C, 5 cm/min) (cm)	/	24.8	57
Softening point (Ring and ball method) (°C)	52	100	91
Elastic restitution (25°C) (%)	/	98	97.5

Table 2. Test results of interlayer oil

Test items	Sample types		
	LFT	GT	RL
Sieve residue (0.3 mm, 25°C) (%)	0.06	0.01	0.02
Viscosity (s)	96	42	40
Evaporation residue, 24 h (%)	79	66	59

**Fig. 1.** Gradations of the three aggregate types.

2.2 Specimens prepare

Marshall samples are made according to T0702-2011 [18], the asphalt mixtures are paved 10 mm-thickness on a 300 mm × 300 mm × 50 mm rutting plate with an SMA25 mixture to formulate the combined rutting plate, and the UAO specimens (100 mm × 100 mm × 60 mm) were cut from the combined rutting plate after 24 hours, as shown in Figure 2. Engraved plates of the same size as UAO specimens and core samples 100 mm in diameter are drilled from the trial sections (as shown in Figure 3).



Fig. 2. Simulated UAO specimens.

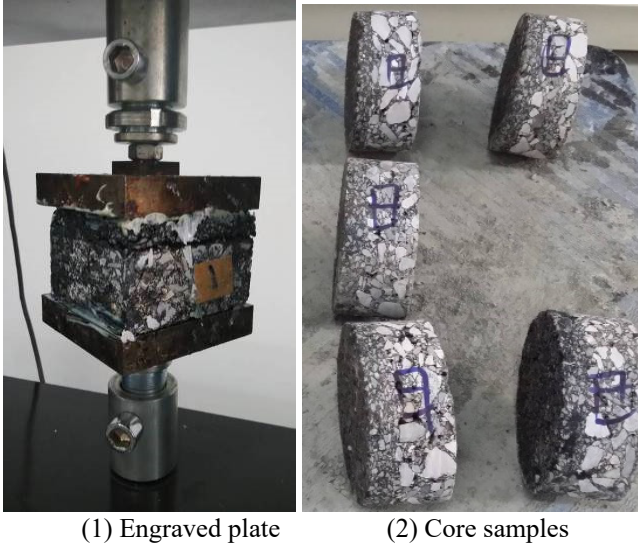


Fig. 3. Specimens from field

2.3 Trial section construction

Three 100 m road sections are chosen for UAO construction, and old pavement conditions are shown in Figure 4. Pavements are crack-sealed before overlay if a crack opening is more than 6.25 mm according to [19]. Asphalt mixture paving is done closely after emulsified asphalt spreading. The spreading width and amount of emulsified asphalt are adjusted according to the pavement condition, and the paving speed of the mixture is adjusted according to the paving thickness. The mixtures are compacted by a double-wheel roller 1 to 2 times, and the times of rolling are no more than 3 to protect the fine aggregates from the crush.

3 Results

3.1 Laboratory evaluation of UAO mixtures

Laboratory tests of the three mixtures.

Marshall stability tests (T0709-2011) are used to verify the basic performance of mixtures. A strong bond between the UAO and the underlying pavement is important to prevent slippage and premature failure of the top layer, higher shear stresses are induced at the interface. End tensile and diagonal shear tests (45°) are conducted on the UAO specimens and core samples to assess the magnitude of bond and shearing resistance, the test methods are shown in Figures 4 and 5. The loading rate of the MTS (mechanical testing simulation) machine is set as the minimum value (2 mm/min) for diagonal shear and end tensile tests, the test results are shown in Table 3 and Figures 4 - 6.



Fig. 4. End tensile tests (from left to right: LFT UAO specimen; LFT core sample; GT UAO specimen; GT core sample; RL UAO specimen; RL core sample.)

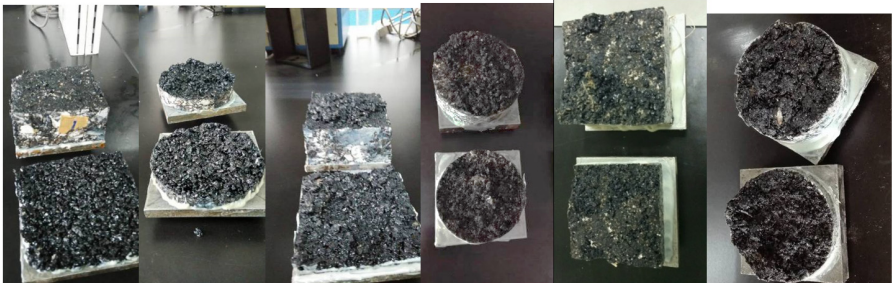


Fig. 5. The damage interfaces of end tensile tests (from left to right: LFT UAO specimen; LFT core sample; GT UAO specimen; GT core sample; RL UAO specimen; RL core sample.)



Fig. 6. Diagonal shear tests (from left to right: test method; an LFT UAO specimen after the test; a GT UAO specimen after the test; an RL UAO specimen after the test.)

Table 3. Laboratory test results of the three mixtures

Number	Test items	Sample types		
		LFT	GT	RL
#1	Marshall stability (KN)	2.25	9.18	12.6
#2	Flow value (0.1 mm)	5.18	3.48	2.54
#3	Diagonal shear strength (KN)	4.88	4.70	4.90
#4	Cantabro stripping (%)	15.1	5.2	4.0
#5	Bond strength of rut plate (30°C) (MPa)	0.0308	0.3560	0.5820
#6	Bond strength of rut plate (50°C) (MPa)	0.0024	0.0476	0.0801
#7	Bond strength of core sample (50°C) (MPa)	0.0222	0.0722	0.0763
#8	Bond strength of core sample (50°C, 15 days) (MPa)	0.0317	0.0894	0.1074

Water stability tests of GT and RL mixtures.

Freeze-thaw splitting tests (T0729-2011 for test method, T0717-2011 for saturated test, T0716-2011 for splitting test at a loading rate of 50 mm/min), and immersion Marshall stability tests (T0709-2011) are used to test the resistance to water damage. The Hamburg Wheel Tracking Device (HWTd) is used to measure the combined effects of rutting and moisture damage by rolling a steel wheel across the surface according to T0733-2011. The specimens are loaded until the number of reciprocations of the steel wheel reaches 20,000 or until the deformation of 20 mm is produced. The moving speed of the steel wheel is about 340 mm/s. All the water stability test results are shown in Table 4.

Table 4. Water stability tests of GT and RL mixtures.

Test items		Test results
Residual stability (%)	GT	94
	RL	88
Splitting strength ratio (TSR)	GT	91
	RL	83
HWTd	12.5mm rolling times	GT 16000

	RL	14000
Stripping inflection point	GT	16163
	RL	7713

3.2 Pavement performance of trial sections

The three trial sections are observed, and the thicknesses of UAOs are measured through core samples drilled. Skid resistance, macrotexture depth, and permeability are investigated to compare the work performance of UAOs, and cycle rutting tests are used to estimate rutting resistance performance.

Surface thickness and condition investigation.

Trial sections in Figures 7 and 8 show the core samples of distress positions, the thickness values measured with core samples are shown in Table 5.



Fig. 7. Pavement condition after one month (from left to right: LFT; GT; RL).

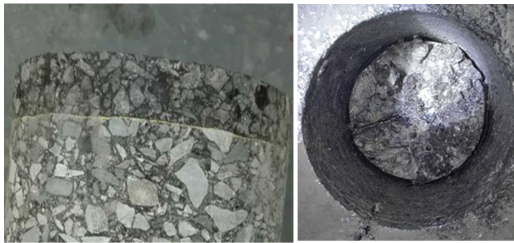


Fig. 8. The core samples at distress positions (from left to right: GT, RL).

Table 5. Surface thickness by measuring core samples (mm)

Specimens	1	2	3	4	5	6	7	8
LFT	11	12	12	12	13	12	11	13
GT	12	11	11	12	13	10	11	12
RL	11	10	11	10	11	10	—	—

After one month, bleeding was found in the GT trial section and a crack occurred in the RL trial section (Figure 5). It can be seen from Figure 5: (1) The bleeding is caused

by the upward migration of excess binder from the tack coat and may be a contributing factor to the loss of skid resistance in the pavements, which is also proved by a previous study of UTBWC [13]. Experience gained is that the quantity control of interlayer oil during the construction of UAO is very important. (2) The reflected crack that occurred provides evidence again that the underlying pavement should be crack-sealed well.

Skid resistance, texture, and permeability.

Skid resistance is related to the pavement's micro and macro texture as noise which is mainly related to macrotexture [20]. MTD (macrotexture depth) measured by sand-laying method (T0961-95), BPN measured by portable pendulum tester (T0964-2008), permeability coefficient measured by water seepage simplifying test (T0971-2008), and maximum clearance measured by three-meters ruler are shown in Figure 9.

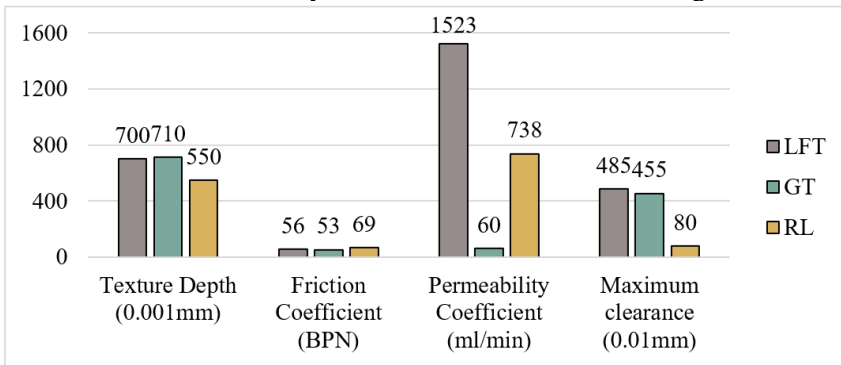


Fig. 9. Infield test results.

Pavement in the field after a short period.

Selected urban road sections (as shown in Table 6) with similar conditions and traffic volume are constructed with RL and GT UAOs. PosiTest Pull-Off Adhesion Tester is used for field tests after 12 months, as the potential failure modes of pavement after UAO treatment are mainly reflected in the shear failure caused by excessive horizontal shear stress in a certain layer or between them.

Before the pull-off test, a test area with a diameter of 5 cm and a depth of about 3 cm should be drilled on the surface, then epoxy glue must be applied after water drying, and the pull-off end element is glued on the test area. After the glue exerts its strength, the instrument is installed on the pull-off end element and the test is carried on. The test procedure is shown in Figure 10, and the horizontal shear stress is calculated according to Formula 3, and test results are shown in Table 7.

$$f_b = \frac{4F_b}{\pi D_f^2} \quad (1)$$

where f_b is the horizontal shear stress, D_f is the diameter of the contact area, and F_b is the maximum pull-off force.



Fig. 10. Pull-off test in the field.

Table 6. Condition of selected road sections before and after UAO construction

Test section	Length (m)	Surface type	AADT	PCI	RD (mm)	IRI	PCI-1	IRI-1
1	433	AC13-4 cm	16840	84.4	3.23	5.07	98	4.31
2	439	AC13-4 cm	19580	82.52	3.59	5.69	98	3.51
3	439	AC13-4 cm	20460	81.31	2.75	4.11	82.83	4.07
4	550	AC13-4 cm	18980	78.32	2.15	8.34	78.14	4.71
5	207	AC13-4 cm	25450	77.95	2.42	4.73	79.54	4.59
6	160.5	AC13-4 cm	20880	83.54	2.29	6.01	80.06	4.41
7	200	AC13-4 cm	24040	80.22	2.30	8.21	89.82	4.24

*-1 represents the test after 2 years

Table 7. Results of pull-off tests on RL & GT UAOs

Test section	Mixture Type	Pull-off strength (MPa)	Remarks
1	GT	0.76	adhesive layer damage
2	GT	0.51	adhesive layer damage
3	GT	0.54	adhesive layer damage
4	RL	0.34	overlay layer failure
5	RL	0.35	overlay layer failure
6	RL	0.33	overlay layer failure
7	RL	0.33	overlay layer failure

4 Discussion

4.1 Comparison of binders, mixtures, and field performance of the three UAOs

Binder properties.

The comparison of the binder properties of the three UAOs is shown in Figure 11.

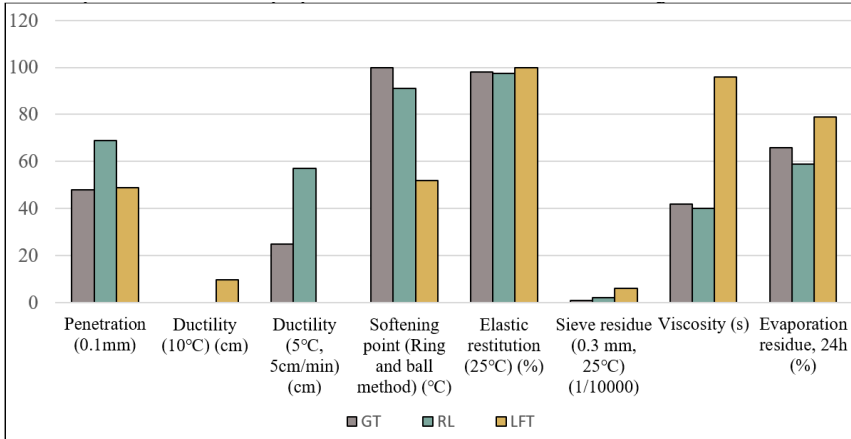


Fig. 11. Comparison of binder properties.

As seen from Figure 11, the strength of GT asphalt is largest at normal temperature, and RL and LFT are equally matched. The comparison result of performance at high temperatures is GT > RL > LFT. The comparison result of performance at low temperatures is RL > GT > LFT. Elastic restitutions are equally matched among the three. For interlayer oil, the comparison results of viscosity values and evaporation residues of interlayer oils used are both LFT > GT > RL. The comparison result of sieve residues (0.3 mm) is LFT > GT > RL. Interlayer oil of LFT is the most excellent one based on the above indexes.

Comparison of mixture properties.

A comparison of the mixture performance of the three UAOs is shown in Figure 12. Negative operation is used in Figure 12 for flow value and Cantabro stripping to visually display the performance difference of all indexes.

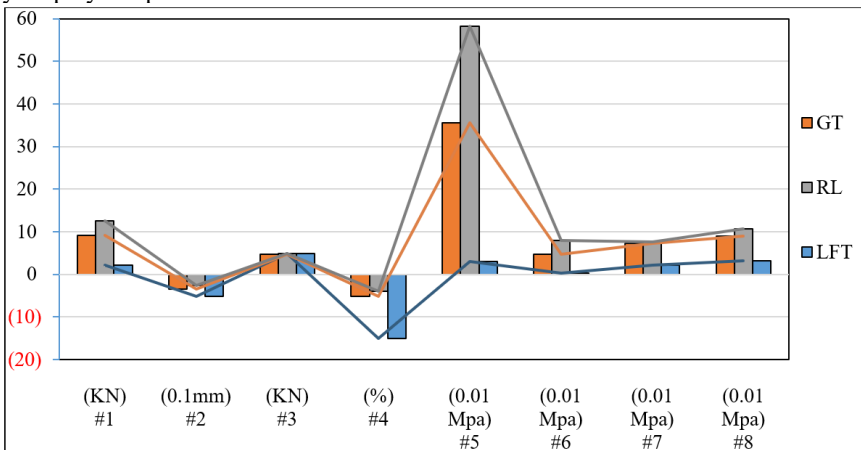


Fig. 12. Comparison of laboratory test results of mixtures of the three UAOs.

It can be seen from Table 3 and Figure 12 that RL mixtures do best at all indexes, and LFT mixtures get the worst performance. The diagonal shear strength values of the three mixtures are very close. The mode of failure is determined by visual inspection and failure within the UAO. In the bottom layer, it is a cohesion failure, failure partly at the interface and partly in the top layer is a mixed failure, and failure at the interface is an adhesion failure [21]. All of the bond damages are cohesion failures in the bottom layer (as seen from core samples and UAO specimens in Figure 5). but the shear damages are all in the adhesion mode (Figure 6). The shear stresses and tensile stresses of the diagonal shear tests can be calculated by (1) and (2).

$$\sigma_{\alpha} = \frac{P}{A} (\cos 45^{\circ} + f \sin 45^{\circ}) \quad (2)$$

$$\tau_{\alpha} = \frac{P}{A} (\cos 45^{\circ} - f \sin 45^{\circ}) \quad (3)$$

where α is the diagonal angle, which is 45° in this test, P is the loading value, A is the sectional area of the specimen, and f is the rolling friction coefficient which is set as 0.003 in this study.

Most of the HMA bond strength tests for interlayers reported in the literature are either direct-shear or tension-based [4]. All bonding strengths at 50°C drop sharply, and the descent ratio is inversely proportional to the pull force, as the ratios (in percent) of bond strength at 50°C to bond strength at 30°C are 1/12.8, 1/7.5, and 1/7.2, the shear stress and tensile stress of LFT measured by diagonal shear tests are about 0.344 MPa and 0.346 MPa respectively, which are much greater than the maximum LFT stress measured by the end tensile test (0.0317 MPa). The strength threshold for adhesion failure is much higher than cohesion failure in the overlay or bottom layer. Besides, Table 4 shows dense-graded mixture is better than a half-open-graded mixture at all water stability test indexes.

Comparison of field performance.

It can be seen from trial section images in Figures 9 and 10 that the LFT trial section performs best after being built, which may be due to its workability during construction with low visibility of binders used at high temperatures. Besides, the average thickness of LFT is 12 mm (Table 4), which is thicker than the other two UAOs. As seen in Figure 7, the MTD of RL is much lower than the other two, BPN of RL is the highest of all. As a low-order macrotexture is beneficial for tire-road noise reduction [25], RL is a preferable solution for both anti-noise and skid resistance. However, the high value of the permeability coefficient makes LFT and RL UAOs need a good interlayer process, which includes well-sealed underlying pavement and good bonding properties. RL also seems to be more suitable for restoring pavement smoothly than LFT and GT, which means that RL can provide better ride quality. Figure 9 shows that the rutting depth (RD) of LFT UAO has a sharp increase, reaching 5 mm after about 80 cycles, by contrast, the RD of RL UAO is less than 1 mm, and the RD of GT has not yet arrived at 2 mm in the same condition. As seen from Figure 10, the aggregate loss is the most serious in LFT UAO, GT has a certain degree of aggregate separation, and RL is characterized by the loss of a few aggregates. RL performs best on both rutting deformation

and stripping resistance. Though it is better on waterproof, GT is not good at anti-deformation and stripping at high temperatures, some traces also can be found by the ability to improve smoothness. The analysis above leads to the conclusion that LFT as an open-graded mixture, cannot anti-stripping or rut. Table 5 and Figure 10 show the pavement conditions and failure mode by pull-off test after 12 months, GT is in adhesion failure mode, and RL is in cohesion failure mode with the overlay. The pull-off strength of GT is higher than 0.5 MPa, it can be inferred that the internal strength of GT UAO is even higher, while the pull-off strength of RL is lower than 0.35 MPa. The pull-off strength of GT is higher than that of RL, which is contrary to the conclusions of previous experiments for both UAO specimens and core samples. As the conditions of the old pavements are similar (as shown in Table 5), these contrary results may be because of the permeability of RL making the RL UAO not dry enough, which also reflects that RL UAO is sensitive to water and may lead to water damage. The pavement quality indexes (PCI and IRI) of road sections also prove this conclusion.

4.2 Analysis of materials used for UAO performance

Binders.

In comprehensive analyses of 4.1.1 and 4.1.2, the high-temperature performance difference between GT and RL seems to have no influence, and only the ductility property at low temperatures is consistent with the mixture performance. However, all the experiments and constructions were carried out in summer (average temperature higher than 30°C), and it can be inferred that asphalt is not the main influence factor for UAO (5 mm to 15 mm) performance. GT mixture has higher water stability than the RL mixture, which may be due to both aggregate gradation and asphalt. Interlay oil property seems negatively related to the bond and shear strengths of core samples or UAO specimens. This may be because the adhesion strength is much higher than the cohesion strength in the overlay, stable interlayer bonding may lead to stress concentration in the overlay. Another study also proved that the type of binder used does not have a great influence on final bond strength [26]. Bond property is not the focus of UAO design.

Aggregate gradations.

As seen in Figure 1, RL has more fine aggregates than the other two mixtures, GT has more 4.75 mm sized aggregates and LFT has more 2.36 mm sized aggregates. Mixture type is a significant factor since a smaller NMAS mixture has higher bond strengths than the coarse-graded, larger NMAS mixture, but significant interactions of mix type (texture) will reverse this trend in some cases [27]. Bonding strengths compared in 4.1.2 support both these two points. The mechanical performance, rutting deformation, and stripping resistance are all dependent on the gradation, as the performance sequence is RL (half-open graded) > GT (dense graded) > LFT (open-graded). And the water stability test results also reflect this point with GT being better than RL. The performance of anti-noise and skid resistance seems to be mainly dependent on the gradation. The ability to restore the pavement smoothness of RL is due to its high content of fine

aggregates. The gradation design of the 4.75-mm NMAS mixture is the key factor of the success of UAO for both service and mechanical performance.

5 Conclusions

This study focused on the constructability and performance of UAO treatments (5mm to 15 mm) with three aggregate types, including open-graded (LFT), half-open-graded (RL), and dense-graded (GT). By comparing the mixture and trial section performance, asphalt and interlayer oil properties are found to have no significant influence on UAO performance, gradation is the main factor. Half open-graded is the most suitable mixture for UAO based on mechanical and serviceability analysis. Water stability test results are consistent with the UAO performance and pull-off results after a short period, which should be further considered during the UAO design. For a rainy area, dense-graded UAO is preferable.

Reference

1. Ye Yu, Lu Sun. Effect of overlay thickness, overlay material, and pre-overlay treatment on evolution of asphalt concrete overlay roughness in LTPP SPS-5 experiment: A multilevel model approach. *Construction and Building Materials* 162 (2018) 192-201
2. Lijun Sun, Chapter 7 - The structural behavior of overlaid asphalt pavements, Editor(s): Lijun Sun, *Structural Behavior of Asphalt Pavements*, Butterworth-Heinemann, 2016, Pages 501-547, ISBN 9780128499085
3. Koohmishi, Mehdi; Palassi, Massoud (2015): Evaluation of Application of Thin HMA Overlay on the Existing Flexible Pavement for High-Traffic-Volume Rural Highways. In *Period. Polytech. Civil Eng.* 59 (1), pp. 65-75. DOI: 10.3311/PPci.7128.
4. Haritha Musty and Mustaque Hossain. Performance of Ultra-Thin Bituminous Overlays. T&DI Congress 2014
5. Sol-Sánchez, M.; García-Travé, G.; Ayar, P.; Moreno-Navarro, F.; Rubio-Gámez, M. C. (2017): Evaluating the mechanical performance of Very Thin Asphalt Overlay (VTAO) as a sustainable rehabilitation strategy in urban pavements. In *Mater. construct.* 67 (327), p. 132. DOI: 10.3989/mc.2017.05016.
6. Dar Hao Chen, Tom Scullion. Very Thin Overlays in Texas, *Construction and Building Materials* 95 (2015) 108-116.
7. Al-Qadi, Imad L. (Ed.) (2013): *Airfield and highway pavement 2013. Sustainable and efficient pavements: proceedings of the 2013 Airfield and Highway Pavement Conference; June 9 - 12, 2013, Los Angeles, California.* American Society of Civil Engineers; Transportation & Development Institute; Airfield and Highway Pavement Conference. Reston, Va.: ASCE.
8. Liu, Ziming; Luo, Sang; Quan, Xun; Wei, Xiaohao; Yang, Xu; Li, Qiang (2019): Laboratory evaluation of the performance of porous ultra-thin overlay. *Construction and Building Materials* 204, pp. 28-40. DOI: 10.1016/j.conbuildmat.2019.01.147.
9. Yichang (James) Tsai, Yi-Ching Wu, April Gadsby and Sheila Hines. Critical Assessment of the Long-Term Performance and Cost-Effectiveness of a New Pavement Preservation Method: Micro-milling and Thin Overlay. *Transportation Research Record: Journal of the Transportation Research Board* 2016 2550: 8-14

10. Im, Soohyok; You, Taesun; Kim, Yong-Rak; Nsengiyumva, Gabriel; Rea, Robert; Haghshenas, Hamzeh (2018): Evaluation of Thin-Lift Overlay Pavement Preservation Practice. Mixture Testing, Pavement Performance, and Lifecycle Cost Analysis. In *J. Transp. Eng., Part B: Pavements* 144 (3), p. 4018037. DOI: 10.1061/JPEODX.0000064.
11. Mansour Solaimanian, Shelley Stoffels, Scott Milander, and Dennis Morian. Evaluation of Thin Hot Mix Asphalt Overlay, FHWA-PA-2016-005-110807
12. Xinjun Li, Nelson Gibson, Xicheng Qi, Trenton Clark, and Kevin McGhee. Laboratory and Full-Scale Evaluation of 4.75-mm Nominal Maximum Aggregate Size Superpave Overlay. *Transportation Research Record: Journal of the Transportation Research Board*, No. 2293, Transportation Research Board of the National Academies, Washington, D.C., 2012, pp. 29-38. DOI: 10.3141/2293-04
13. J. F. Muñoz, C. Balachandran, Y. Yao, A. Shastry, L. Perry, M. A. Beyene & T. Arnold (2018) Forensic investigation of the cause(s) of slippery ultra-thin bonded wearing course of an asphalt pavement: influence of binder content, *International Journal of Pavement Engineering*, 19:7, 593-600, DOI: 10.1080/10298436.2016.1199870
14. Wang, George; Smith, Gregory; Shores, Richard (2012): Pavement noise investigation on North Carolina highways. An on-board sound intensity approach. In *Can. J. Civ. Eng.* 39 (8), pp. 878-886. DOI: 10.1139/I2012-076.
15. Garcia-Gil L, Miró R, Pérez-Jiménez FE. Evaluating the Role of Aggregate Gradation on Cracking Performance of Asphalt Concrete for Thin Overlays. *Applied Sciences*. 2019; 9(4):628-640.
16. Songsu Son, Imad L. Al-Qadi & Tom Zehr (2016) 4.75 mm SMA Performance and Cost-Effectiveness for Asphalt Thin Overlays, *International Journal of Pavement Engineering*, 17:9, 799-809, DOI: 10.1080/10298436.2015.1019500
17. James, R., A. Cooley, and S. Buchanan. Development of Mix Design Criteria for 4.75-mm SUPERPAVE Mixes. In *Transportation Research Record: Journal of the Transportation Research Board*, No. 1819, Transportation Research Board of the National Academies, Washington, D.C., 2003, pp. 125-133.
18. Ministry of Transport of the People's Republic of China. Standard Test Methods of Bitumen and Bituminous Mixtures for Highway Engineering, JTG E20-2011, 2011-9-13.
19. L.F. Walubita, T. Scullion, Thin HMA Overlays in Texas: Mix Design and Laboratory Material Property Characterization. *TxDOT Report 0-5598-1*, Texas, USA, 2008.
20. Reginald B. Kogbara, Eyad A. Masad, Emad Kassem, A. (Tom) Scarpas, Kumar Anupam. A state-of-the-art review of parameters influencing measurement and modeling of skid resistance of asphalt pavements, *Construction and Building Materials*, Volume 114, 2016, Pages 602-617.
21. Alexandra Destrée & Joëlle De Visscher (2017) Impact of tack coat application conditions on the interlayer bond strength, *European Journal of Environmental and Civil Engineering*, 21:sup1, 3-13.
22. Muñoz J. F, Balachandran C., Yao Y., Shastry A.; Perry, L., Beyene M. A., Arnold T. (2016). Forensic investigation of the cause(s) of slippery ultra-thin bonded wearing course of an asphalt pavement. Influence of binder content. In *International Journal of Pavement Engineering* 19 (7), pp.593-600.
23. A.C. Collop, M.H. Sutanto, G.D. Airey, R.C. Elliott. Shear bond strength between asphalt layers for laboratory prepared samples and field cores, *Construction and Building Materials*, Volume 23, Issue 6, 2009, Pages 2251-2258.
24. A.C. Raposeiras, D. Castro-Fresno, A. Vega-Zamanillo, J. Rodriguez-Hernandez. Test methods and influential factors for analysis of bonding between bituminous pavement layers, *Construction and Building Materials*, Volume 43, 2013, Pages 372-381.

25. Ahammed, M. Alauddin; Tighe, Susan L. Pavement surface friction and noise. Integration into the pavement management system. In *Can. J. Civ. Eng.* 2010, 37 (10), pp. 1331–1340. DOI: 10.1139/L10-076.
26. R.C. West, J. Zhang, J. Moore, Evaluation of Bond Strength between Pavement Layers. NCAT Report, National Center for Asphalt Technology, Auburn, AL, 2005, pp. 05-08.
27. Francesco Canestrari, Gilda Ferrotti, Manfred Partl, and Ezio Santagata. Advanced Testing and Characterization of Interlayer Shear Resistance, Transportation Research Record: Journal of the Transportation Research Board 2005, 1929: 69-78.

Open Access This chapter is licensed under the terms of the Creative Commons Attribution-NonCommercial 4.0 International License (<http://creativecommons.org/licenses/by-nc/4.0/>), which permits any noncommercial use, sharing, adaptation, distribution and reproduction in any medium or format, as long as you give appropriate credit to the original author(s) and the source, provide a link to the Creative Commons license and indicate if changes were made.

The images or other third party material in this chapter are included in the chapter's Creative Commons license, unless indicated otherwise in a credit line to the material. If material is not included in the chapter's Creative Commons license and your intended use is not permitted by statutory regulation or exceeds the permitted use, you will need to obtain permission directly from the copyright holder.

